

Picosecond Third-Harmonic Light Generation in β -BaB₂O₄

P. Qiu* and A. Penzkofer

Naturwissenschaftliche Fakultät II – Physik, Universität, D-8400 Regensburg,
Fed. Rep. Germany

Received 29 September 1987/Accepted 19 January 1988

Abstract. The type-II phase-matched third-harmonic light generation in a β -BaB₂O₄ crystal is studied experimentally. A passively mode-locked Nd: phosphate glass laser is used as a pump source. At a pump pulse peak intensity of $I_{10} = 5 \times 10^{10}$ W/cm² a third-harmonic conversion efficiency of a percent is obtained. A theoretical discussion of phase-matched third-harmonic generation in crystals of the symmetry group of β -BaB₂O₄ (trigonal class 3) is given. The effective nonlinear susceptibility χ_{eff} for type-II phase-matching is determined.

PACS: 42.65C

β -BaB₂O₄ (BBO) is an excellent nonlinear optical crystal for second-order nonlinear optical applications like second-harmonic generation, three-photon frequency mixing, and parametric three-photon interaction [1–9]. The wide transparency region (190–2500 nm), the large second-order nonlinear susceptibility and the high damage threshold make this crystal superior to KDP and ADP [1–9]. The small group-velocity mismatch of the crystal is attractive in the femtosecond region [5].

In this paper we study the third-harmonic generation in a β -BaB₂O₄ crystal. Single picosecond pulses of a passively mode-locked Nd: phosphate glass laser are used as pump source. The type-II phase-matching is chosen (o \rightarrow e interaction, o indicates the ordinary ray and e the extraordinary ray).

β -BaB₂O₄ is a negative uniaxial crystal (extraordinary refractive index $n_e <$ ordinary refractive index n_o) of the trigonal crystal class (space group R3, point group 3 [1, 2]). The crystal has no inversion center. In the crystal light generation at the third-harmonic frequency, $\omega_3 = 3\omega_1$, may occur by cascading second-order nonlinear optical effects (second-harmonic generation, $\omega_1 + \omega_1 \rightarrow \omega_2$, and frequency mixing, $\omega_2 + \omega_1 \rightarrow \omega_3$) or by a direct third-order nonlinear optical process (direct third-harmonic generation, $\omega_1 + \omega_1 + \omega_1 \rightarrow \omega_3$) [10, 11].

* On leave from the Shanghai Institute of Optics and Fine Mechanics, Academia Sinica, Shanghai, P.R. China

In the theoretical discussion the various phase-matched cascading processes and direct third-harmonic generation processes are analysed. The experiments are restricted to the type-II phase-matched third-harmonic generation.

1. Theory

In a recent paper the phase-matched third-harmonic generation in calcite has been analysed [12]. In contrast to β -BaB₂O₄, calcite is an uniaxial crystal with inversion symmetry (trigonal crystal class, space group R3c, point group 3m) and therefore no second-order nonlinear optical processes contribute to the third-harmonic generation. Here, the theory of [12] is extended to include the second-order cascade processes to the light generation at the third-harmonic frequency in β -BaB₂O₄.

The light propagation through the crystal is depicted in Fig. 1. Only phase-matched collinear interaction is considered. The x-, y-, and z-axes represent the crystal-fixed rectangular coordinate system. The optical axis is parallel to the z-axis. The (X, Y, Z) system is the laboratory-fixed rectangular coordinate system. The wave propagation in the (XYZ) system is characterized by the wave vectors $\mathbf{k}_1 \parallel \mathbf{k}_2 \parallel \mathbf{k}_3 \parallel Z$ -axis, the ordinary field strength $\mathbf{E}_o \parallel X$ -axis and the extraordinary dielectric displacement $\mathbf{D}_e \parallel Y$ -axis [13]. In the (x, y, z)-coordinate system the unit vector of the ordi-

Table 1. Cascading third harmonic generation and direct third-harmonic generation in β -BaB₂O₄. Pump wavelength $\lambda_1 = 1.054 \mu\text{m}$

Interaction	θ_{PM} [°]	Δk [cm ⁻¹]	α_1 [°]	α_2	α_3	β	$F(\beta)$
<i>Pure cascading processes</i>							
Phase-matched second-harmonic generation ($\Delta k_{\text{SHG}} = 0$)							
$o_1 o_1 \rightarrow e_2$	22.93	0	3.12	3.21	3.42		
$e_2 o_1 \rightarrow e_3$		5413.7				0	$\cos^6 \beta$
$e_2 e_1 \rightarrow e_3$	—	6557.7				26.57	$\cos^4 \beta \sin^2 \beta$
$e_2 o_1 \rightarrow o_3$	—	9293.3				0	$\cos^6 \beta$
$e_2 e_1 \rightarrow o_3$	—	10437.4				26.57	$\cos^4 \beta \sin^2 \beta$
$o_1 e_1 \rightarrow e_2$	33.06	0	3.89	3.99	4.25		
$e_2 o_1 \rightarrow e_3$		4032.5				26.57	$\cos^4 \beta \sin^2 \beta$
$e_2 e_1 \rightarrow e_3$	—	6237.5				63.43	$\cos^2 \beta \sin^4 \beta$
$e_2 o_1 \rightarrow o_3$	—	11498.4				26.47	$\cos^4 \beta \sin^2 \beta$
$e_2 e_1 \rightarrow o_3$	—	13703.4				63.43	$\cos^2 \beta \sin^4 \beta$
Phase-matched frequency mixing ($\Delta k_{\text{FM}} = 0$)							
$e_2 o_1 \rightarrow e_3$	60.52	0	3.41	3.50	3.70		
$o_1 o_1 \rightarrow e_2$	—	8715				0	$\cos^6 \beta$
$o_1 e_1 \rightarrow e_2$	—	3372.2				26.57	$\cos^4 \beta \sin^2 \beta$
$e_1 e_1 \rightarrow e_2$	—	1970.64				63.43	$\cos^4 \beta \sin^4 \beta$
$o_2 o_1 \rightarrow e_3$	31.61	0	3.81	3.91	4.16		
$o_1 o_1 \rightarrow o_2$	—	2380				0	$\cos^6 \beta$
$o_1 e_1 \rightarrow o_2$	—	4421.4				26.57	$\cos^4 \beta \sin^2 \beta$
$e_1 e_1 \rightarrow o_2$	—	6462.7				63.43	$\cos^2 \beta \sin^4 \beta$
$o_2 e_1 \rightarrow e_3$	38.99	0	4.10	4.20	4.47		
$o_1 o_1 \rightarrow o_2$	—	2380				26.57	$\cos^4 \beta \sin^2 \beta$
$o_1 e_1 \rightarrow o_2$	—	5281.8				63.43	$\cos^2 \beta \sin^4 \beta$
$e_1 e_1 \rightarrow o_2$	—	8183.7				90	$\sin^6 \beta$
<i>Mixed direct third-harmonic generation and cascading processes</i>							
Phase-matched third harmonic generation ($\Delta k_{\text{THG}} = \Delta k_{\text{SHG}} + \Delta k_{\text{FM}} = 0$) ^a							
type-I							
$o_1 o_1 o_1 \rightarrow e_3$	37.69	0	4.07	4.17	4.44	0	$\cos^6 \beta$
$o_1 o_1 \rightarrow e_2 o_1 \rightarrow e_3$	—	3330.5				0	$\cos^6 \beta$
$o_1 o_1 \rightarrow o_2 o_1 \rightarrow e_3$	—	2380.0				0	$\cos^6 \beta$
type-II							
$o_1 o_1 e_1 \rightarrow e_3$	47.40	0	4.09	4.19	4.45	26.57	$\cos^4 \beta \sin^2 \beta$
$o_1 o_1 \rightarrow e_2 e_1 \rightarrow e_3$	—	5742.1				26.57	$\cos^4 \beta \sin^2 \beta$
$o_1 o_1 \rightarrow o_2 e_1 \rightarrow e_3$	—	2380.0				26.57	$\cos^4 \beta \sin^2 \beta$
$o_1 e_1 \rightarrow e_2 o_1 \rightarrow e_3$	—	1833.2				26.57	$\cos^4 \beta \sin^2 \beta$
$o_1 e_1 \rightarrow o_2 o_1 \rightarrow e_3$	—	6288.9				26.57	$\cos^4 \beta \sin^2 \beta$
type-III							
$o_1 e_1 e_1 \rightarrow e_3$	84.33	0	0.76	0.78	0.82	64.43	$\cos^2 \beta \sin^4 \beta$
$o_1 e_1 \rightarrow e_2 e_1 \rightarrow e_3$	—	4949.1				64.43	$\cos^2 \beta \sin^4 \beta$
$o_1 e_1 \rightarrow o_2 e_1 \rightarrow e_3$	—	9195.4				64.43	$\cos^2 \beta \sin^4 \beta$
$e_1 e_1 \rightarrow e_2 o_1 \rightarrow e_3$	—	1866.4				64.43	$\cos^2 \beta \sin^4 \beta$
$e_1 e_1 \rightarrow o_2 o_1 \rightarrow e_3$	—	16010.9				64.43	$\cos^2 \beta \sin^4 \beta$

^a Δk_{FM} is listed for cascading contributions

generation and the frequency mixing is not possible in a single crystal. The light generation at the third-harmonic frequency by phase-matched second-harmonic generation and phase-matched frequency mixing is only possible by the successive application of two crystals which are differently oriented [14, 15]. The application of two separately phase-matched

crystals is experimentally more complex than the application of a single crystal, but the light generation is more efficient with two phase-matched crystals.

For the direct third-harmonic generation the process $\omega_1 + \omega_1 + \omega_1 \rightarrow \omega_3$ is phase-matched by

$$\Delta k_{\text{THG}} = k_3 - k_{1a} - k_{1b} - k_{1c} = 0. \quad (5c)$$

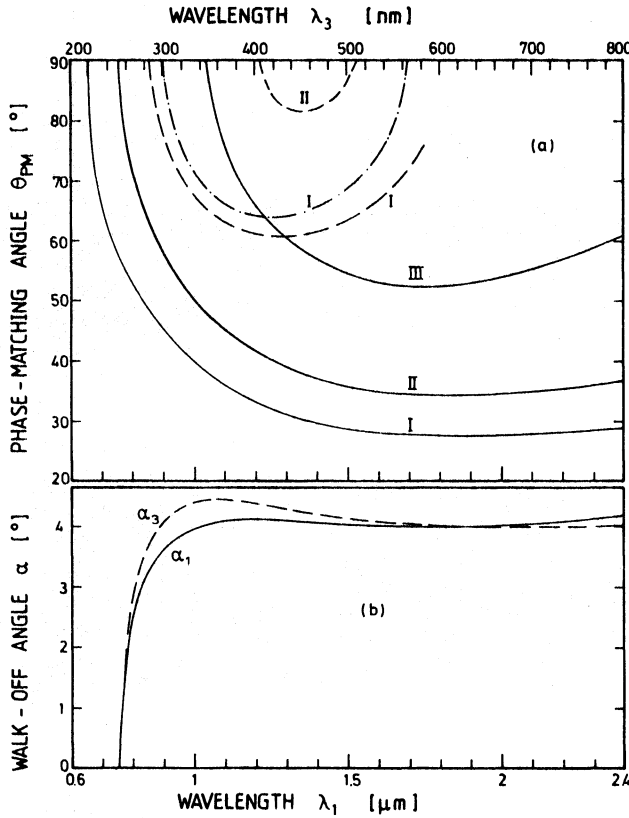


Fig. 3. (a) Phase-matching angles θ_{PM} versus wavelength λ_1 and λ_3 for type-I (ooo \rightarrow e), type-II (ooe \rightarrow e), and type-III (oee \rightarrow e) interaction. Solid curves: $\beta\text{-BaB}_2\text{O}_4$. Dashed curves: KDP. Dash-dotted curve: ADP. (b) Walk-off angles α_1 and α_3 versus wavelength λ_1 and λ_3 for type-II phase-matched interaction in $\beta\text{-BaB}_2\text{O}_4$.

The contributing cascading second-order processes (Table 1) are characterized by

$$\Delta k_{SHG} + \Delta k_{FM} = \Delta k_{THG} = 0. \quad (5d)$$

The wave-vector diagrams for $\Delta k_{SHG} = 0$ (a), $\Delta k_{FM} = 0$ (b), and $\Delta k_{THG} = 0$ (c) are inserted in Fig. 2. The phase-matching angles versus wavelength are plotted in Fig. 3a for type-I (ooo \rightarrow e), type-II (ooe \rightarrow e), and type-III (oee \rightarrow e) mixed direct and cascading third-harmonic generation in $\beta\text{-BaB}_2\text{O}_4$. For comparison the phase-matching curves of KDP (dashed curves, only type-I and type-II phase-matching possible) and of ADP (dash-dotted curve, only type-I phase-matching possible) are included (refractive index data from [16]).

The walk-off angle α between energy flow direction (ray direction) \mathbf{s} and wavevector direction \mathbf{k} (Fig. 1) of extraordinary polarized light is given by [17]

$$\tan \alpha = \frac{1}{2} \sin(2\theta) n_e^2(\theta) \left(\frac{1}{n_e^2} - \frac{1}{n_o^2} \right). \quad (6)$$

In Fig. 3b the walk-off angles α_1 and α_3 versus wavelength are shown for the type-II third-harmonic

generation process in $\beta\text{-BaB}_2\text{O}_4$. The walk-off angles are listed in Table 1 for the various interaction processes at $\lambda_1 = 1.054 \mu\text{m}$.

For the cascading third-harmonic generation and the direct third-harmonic generation the relevant equations are derived in the following [10]. The wave equation is given by [17–19]

$$\nabla \times \nabla \times \mathbf{E} + \frac{\tilde{\epsilon}}{c_0^2} \frac{\partial^2}{\partial t^2} \mathbf{E} = -\mu_0 \frac{\partial^2}{\partial t^2} \mathbf{P}_{NL}, \quad (7)$$

being $\tilde{\epsilon}$ the relative permittivity tensor, c_0 the vacuum light velocity, and μ_0 the vacuum permeability. Solutions of (7) are found by the plane wave ansatz

$$\mathbf{E} = \frac{1}{2} (E_1 e^{i(\omega_1 t - k_1 Z)} \mathbf{e}_1 + E_2 e^{i(\omega_2 t - k_2 Z)} \mathbf{e}_2 + E_3 e^{i(\omega_3 t - k_3 Z)} \mathbf{e}_3 + \text{c.c.}), \quad (8a)$$

$$\mathbf{P}_{NL} = \frac{1}{2} (\mathbf{P}_{NL,1} e^{i(\omega_1 t - k_1^p Z)} + \mathbf{P}_{NL,SHG} e^{i(\omega_2 t - k_2^p Z)} + \mathbf{P}_{NL,FM} e^{i(\omega_3 t - k_3^p Z)} + \mathbf{P}_{NL,THG} e^{i(\omega_3 t - k_3^p Z)} + \text{c.c.}). \quad (8b)$$

Pump pulse depletion is neglected. The slowly varying amplitude approximation leads to [17–20]

$$k_2 \cos^2 \alpha_2 \frac{\partial E_2}{\partial Z} + \frac{\omega_2}{c_0^2} \mathbf{e}_2 \tilde{\epsilon}_2 \mathbf{e}_2 \frac{\partial E_2}{\partial t} = -i \frac{\mu_0 \omega_2^2}{2} \mathbf{e}_2 \mathbf{P}_{NL,SHG} e^{i \Delta k_{SHG} Z}, \quad (9a)$$

$$k_3 \cos^2 \alpha_3 \frac{\partial E_{3,FM}}{\partial Z} + \frac{\omega_3}{c_0^2} \mathbf{e}_3 \tilde{\epsilon}_3 \mathbf{e}_3 \frac{\partial E_{3,FM}}{\partial t} = -i \frac{\mu_0 \omega_3^2}{2} \mathbf{e}_3 \mathbf{P}_{NL,FM} e^{i \Delta k_{FM} Z} \quad (9b)$$

and

$$k_3 \cos^2 \alpha_3 \frac{\partial E_{3,THG}}{\partial Z} + \frac{\omega_3}{c_0^2} \mathbf{e}_3 \tilde{\epsilon}_3 \mathbf{e}_3 \frac{\partial E_{3,THG}}{\partial t} = -i \frac{\mu_0 \omega_3^2}{2} \mathbf{e}_3 \mathbf{P}_{NL,THG} e^{i \Delta k_{THG} Z}. \quad (9c)$$

The nonlinear polarizations are given by [21]

$$\mathbf{P}_{NL,SHG} = 2\epsilon_0 \tilde{\chi}^{(2)} : \mathbf{E}\mathbf{E} = \epsilon_0 E_{1a} E_{1b} \tilde{\chi}^{(2)}(-\omega_2; \omega_1, \omega_1) : \mathbf{e}_{1a} \mathbf{e}_{1b}, \quad (10a)$$

$$\mathbf{P}_{NL,FM} = 2\epsilon_0 \tilde{\chi}^{(2)} : \mathbf{E}\mathbf{E} = 2\epsilon_0 E_2 E_{1c} \tilde{\chi}^{(2)}(-\omega_3; \omega_2, \omega_1) : \mathbf{e}_2 \mathbf{e}_{1c}, \quad (10b)$$

and

$$\mathbf{P}_{NL,THG} = 4\epsilon_0 \tilde{\chi}^{(3)} : \mathbf{E}\mathbf{E}\mathbf{E} = \epsilon_0 E_{1a} E_{1b} E_{1c} \tilde{\chi}^{(3)}(-\omega_3; \omega_1, \omega_1, \omega_1) : \mathbf{e}_{1a} \mathbf{e}_{1b} \mathbf{e}_{1c} \quad (10c)$$

$E_{1a} = E_{1a}e_{1a}$, $E_{1b} = E_{1b}e_{1b}$, and $E_{1c} = E_{1c}e_{1c}$ are the components of the electric field strength, E_1 , that give phase-matching (see below). The wave vectors of the nonlinear polarizations are $k_2^p = k_{1a} + k_{1b}$, $k_{FM}^p = k_2 + k_{1c}$, and $k_3^p = k_{1a} + k_{1b} + k_{1c}$. Transformations to the moving frame ($t' = t - e_2 \tilde{e}_2 e_2 / (c_0 n_2 \cos^2 \alpha_2)$) $\times Z \simeq t - [e_3 \tilde{e}_3 e_3 / (c_0 n_3 \cos^2 \alpha_3)]Z$, and $Z' = Z$) give

$$\frac{\partial E_2}{\partial Z'} = -i \frac{\omega_2}{2n_3 c_0 \cos^2 \alpha_2} \chi_{\text{eff,SHG}}^{(2)} E_{1a} E_{1b} e^{i \Delta k_{\text{SHG}} Z'}, \quad (11a)$$

$$\frac{\partial E_{3,FM}}{\partial Z'} = -i \frac{\omega_3}{n_3 c_0 \cos^2 \alpha_3} \chi_{\text{eff,FM}}^{(2)} E_2 E_{1c} e^{i \Delta k_{FM} Z'}, \quad (11b)$$

and

$$\begin{aligned} \frac{\partial E_{3,THG}}{\partial Z'} \\ = -i \frac{\omega_3}{2n_3 c_0 \cos^2 \alpha_3} \chi_{\text{eff,THG}}^{(3)} E_{1a} E_{1b} E_{1c} e^{i \Delta k_{THG} Z'}. \end{aligned} \quad (11c)$$

The effective nonlinear susceptibilities are

$$\chi_{\text{eff,SHG}}^{(2)} = e_2 \cdot \tilde{\chi}^{(2)} : e_{1a} e_{1b}, \quad (12a)$$

$$\chi_{\text{eff,FM}}^{(2)} = e_3 \cdot \tilde{\chi}^{(2)} : e_2 e_{1c}, \quad (12b)$$

$$\chi_{\text{eff,THG}}^{(3)} = e_3 \cdot \tilde{\chi}^{(3)} : e_{1a} e_{1b} e_{1c}. \quad (12c)$$

The second-order nonlinear susceptibility tensor $\tilde{\chi}^{(2)}$ and the third-order nonlinear susceptibility tensor $\tilde{\chi}^{(3)}$ of β -BaB₂O₄ are listed in Table 2 [17, 22, 23]. The effective nonlinear susceptibilities of the various interaction processes are compiled in Table 3 [12, 22, 23].

The solution of (11a) is

$$\begin{aligned} E_2(Z') = -i \frac{\omega_2}{2n_3 c_0 \cos^2 \alpha_2} \\ \times \chi_{\text{eff,SHG}}^{(2)} E_{1a} E_{1b} \frac{\exp(i \Delta k_{\text{SHG}} Z') - 1}{i \Delta k_{\text{SHG}}} \end{aligned} \quad (13)$$

for $E_2(0) = 0$ (walk-off is neglected). Insertion of (13) into (11b) gives (walk-off is neglected)

$$\begin{aligned} E_{3,FM}(Z') = \frac{\omega_2 \omega_3 \chi_{\text{eff,SHG}}^{(2)} \chi_{\text{eff,FM}}^{(2)}}{2n_2 n_3 c_0^2 \cos^2 \alpha_2 \cos^2 \alpha_3} E_{1a} E_{1b} E_{1c} \\ \times \frac{1}{\Delta k_{\text{SHG}}} \left(\frac{\exp[i(\Delta k_{\text{SHG}} + \Delta k_{FM})Z'] - 1}{\Delta k_{\text{SHG}} + \Delta k_{FM}} \right. \\ \left. - \frac{\exp(i \Delta k_{FM} Z') - 1}{\Delta k_{FM}} \right). \end{aligned} \quad (14)$$

For $\Delta k_{FM} \rightarrow 0$ (phase-matched frequency mixing) (14) reduces to

$$\begin{aligned} E_{3,FM}(Z') = -i \frac{\omega_2 \omega_3 \chi_{\text{eff,SHG}}^{(2)} \chi_{\text{eff,FM}}^{(2)}}{2n_2 n_3 c_0^2 \cos^2 \alpha_2 \cos^2 \alpha_3} \\ \times E_{1a} E_{1b} E_{1c} \frac{Z'}{\Delta k_{\text{SHG}}} \exp(i \Delta k_{FM} Z'/2) \\ \times \frac{\sin(\Delta k_{FM} Z'/2)}{\Delta k_{FM} Z'/2} \end{aligned} \quad (15a)$$

with $\sin(\Delta k_{FM} Z'/2) / (\Delta k_{FM} Z'/2) \rightarrow 1$.

For $\Delta k_{\text{SHG}} \rightarrow 0$ (phase-matched second-harmonic generation) Eq. (14) gives

$$\begin{aligned} E_{3,FM}(Z') = -i \frac{\omega_2 \omega_3 \chi_{\text{eff,SHG}}^{(2)} \chi_{\text{eff,FM}}^{(2)}}{2n_2 n_3 c_0^2 \cos^2 \alpha_2 \cos^2 \alpha_3} \\ \times E_{1a} E_{1b} E_{1c} \frac{Z'}{\Delta k_{FM}} \exp(i \Delta k_{FM} Z'/2) \\ \times \frac{\sin(\Delta k_{FM} Z'/2)}{\Delta k_{FM} Z'/2} \end{aligned} \quad (15b)$$

with $\sin(\Delta k_{FM} Z'/2) / (\Delta k_{FM} Z'/2) \ll 1$. A comparison of (15a) and (16a) shows that the third-harmonic generation via phase-matched second-harmonic generation is negligibly small compared to third-harmonic generation via phase-matched frequency mixing.

In case of $\Delta k_{\text{SHG}} + \Delta k_{FM} = \Delta k_{\text{THG}} \rightarrow 0$ (cascading contribution to direct third-harmonic generation)

Table 2. Second- and third-order nonlinear susceptibility tensors of β -BaB₂O₄ (point group 3). Kleinman symmetry conjecture [24] is assumed

$$\tilde{\chi}^{(2)} = \begin{pmatrix} d_{11} & -d_{11} & 0 & 0 & d_{15} & -d_{22} \\ -d_{22} & d_{22} & 0 & d_{15} & 0 & -d_{11} \\ d_{15} & d_{15} & d_{33} & 0 & 0 & 0 \end{pmatrix}$$

$$\begin{matrix} 1=x \\ 2=y \\ 3=z \end{matrix}$$

$$\tilde{\chi}^{(3)} = \begin{pmatrix} \chi_{11} & 0 & 0 & 0 & \chi_{15} & \chi_{16} & -\chi_{15} & \frac{1}{3}\chi_{11} & 0 & \chi_{10} \\ 0 & \chi_{11} & 0 & \chi_{16} & -\chi_{10} & 0 & \chi_{10} & 0 & \frac{1}{3}\chi_{11} & \chi_{15} \\ -\chi_{15} & -\chi_{10} & \chi_{33} & 0 & \chi_{16} & 0 & \chi_{16} & \chi_{15} & \chi_{10} & 0 \end{pmatrix}$$

$$\begin{matrix} 1=xxx & 2=yyy & 3=zzz & 4=yzz & 5=yyz & 6=xzz & 7=xxz & 8=xyy & 9=xyx & 0=xyz \end{matrix}$$

Eq. (14) simplifies to

$$E_{3,FM}(Z') = -i \frac{\omega_2 \omega_3 \chi_{eff,SHG}^{(2)} \chi_{eff,FM}^{(2)}}{2n_2 n_3 c_0^2 \cos^2 \alpha_2 \cos^2 \alpha_3} \times E_{1a} E_{1b} E_{1c} \frac{Z'}{\Delta k_{FM}} \exp(i \Delta k_{THG} Z'/2) \times \frac{\sin(\Delta k_{THG} Z'/2)}{\Delta k_{THG} Z'/2} \quad (15c)$$

with $\sin(\Delta k_{THG} Z'/2)/(\Delta k_{THG} Z'/2) \rightarrow 1$. $E_{3,FM}$ of (15a) ($\Delta k_{FM} \rightarrow 0$) and $E_{3,FM}$ of (15c) ($\Delta k_{THG} \rightarrow 0$) are of the same magnitude.

The solution of (11c) is (walk-off is neglected)

$$E_{3,THG}(Z') = -i \frac{\omega_3 \chi_{eff,THG}^{(3)} Z'}{2n_3 c_0 \cos^2 \alpha_3} \times E_{1a} E_{1b} E_{1c} \exp(i \Delta k_{THG} Z'/2) \frac{\sin(\Delta k_{THG} Z'/2)}{\Delta k_{THG} Z'/2}. \quad (16)$$

For $\Delta k_{THG} \rightarrow 0$ (phase-matched direct third-harmonic generation) it is $\sin(\Delta k_{THG} Z'/2)/(\Delta k_{THG} Z'/2) \rightarrow 1$.

The total third-harmonic signal is the sum over the various simultaneously phase-matched processes of Table 1 (same phase-matching angle). It may be written as

$$E_3(Z') = -i \frac{\omega_3 Z'}{2n_3 c_0 \cos^2 \alpha_3} \chi_{eff} E_{1a} E_{1b} E_{1c} \times \exp(i \Delta k' Z'/2) \frac{\sin(\Delta k' Z'/2)}{\Delta k' Z'/2} \quad (17)$$

with

$$\chi_{eff} = \sum_{i=1}^m \chi_{eff,i}. \quad (18)$$

The sum runs over the simultaneously phase-matched processes. For phase-matched frequency-mixing interaction ($\Delta k_{FM} \rightarrow 0$) it is

$$\chi_{eff,i} = \frac{\omega_2 \chi_{eff,SHG,i}^{(2)} \chi_{eff,FM,i}^{(2)}}{n_2 c_0 \cos^2(\alpha_2) \Delta k_{SHG}} \quad (19a)$$

and

$$\Delta k' = \Delta k_{FM}.$$

For phase-matched second-harmonic generation ($\Delta k_{SHG} \rightarrow 0$) it is

$$\chi_{eff,i} = \frac{\omega_2 \chi_{eff,SHG,i}^{(2)} \chi_{eff,FM,i}^{(2)}}{n_2 c_0 \cos^2(\alpha_2) \Delta k_{FM}} \quad (19b)$$

and

$$\Delta k' = \Delta k_{FM}.$$

For mixed direct and cascade third-harmonic generation ($\Delta k_{SHG} + \Delta k_{FM} = \Delta k_{THG} \rightarrow 0$) it is (m' number of

phase-matched cascade processes)

$$\chi_{eff} = \chi_{eff,THG}^{(3)} + \chi_{eff,cas} = \chi_{eff,THG}^{(3)} + \sum_{i=1}^{m'} \frac{\omega_2 \chi_{eff,SHG,i}^{(2)} \chi_{eff,FM,i}^{(2)}}{n_2 c_0 \cos^2(\alpha_2) \Delta k_{FM}} \quad (19c)$$

and

$$\Delta k' = \Delta k_{THG}.$$

The third-harmonic intensity generated in a crystal of length l is obtained by use of the relations $I_i = (n_i \epsilon_0 c_0 / 2) |E_i|^2$ ($i = 1, 3$). The result is

$$I_3(l) = \frac{\omega_3^2 l^2}{n_3 n_{1a} n_{1b} n_{1c} c_0^4 \epsilon_0^2 \cos^4 \alpha_3} \times |\chi_{eff}|^2 I_{1a} I_{1b} I_{1c} \frac{\sin^2(\Delta k' l / 2)}{(\Delta k' l / 2)^2}. \quad (20)$$

The electrical field strengths E_{1a} , E_{1b} , and E_{1c} are the ordinary and extraordinary field components according to the interaction processes of Table 1. For example the field components for the type-II phase-matched third-harmonic generation (ooe \rightarrow e) are $E_{1a} = E_{1b} = E_1^o = \cos(\beta) E_1$ and $E_{1c} = E_1^e = \sin(\beta) E_1$ (Fig. 1). The corresponding intensities are $I_{1a} = I_{1b} = I_1^o = \cos^2(\beta) I_1$ and $I_{1c} = I_1^e = \sin^2(\beta) I_1$. For Gaussian pulses the field strengths and the intensities are

$$E_1^o(X, Y, t') = \cos(\beta) E_{10} \exp\left(-\frac{X^2 + Y^2}{2r_0^2}\right) \exp\left(-\frac{t'^2}{2t_0^2}\right), \quad (21a)$$

$$E_1^e(X, Y, Z, t') = \sin(\beta) E_{10} \times \exp\left(-\frac{X^2 + (Y + \alpha_1 Z)^2}{2r_0^2}\right) \exp\left(-\frac{t'^2}{2t_0^2}\right), \quad (21b)$$

$$I_1^o(X, Y, t') = \cos^2(\beta) I_{10} \exp\left(-\frac{X^2 + Y^2}{r_0^2}\right) \exp\left(-\frac{t'^2}{t_0^2}\right), \quad (21c)$$

$$I_1^e(X, Y, Z, t') = \sin^2(\beta) I_{10} \times \exp\left(-\frac{X^2 + (Y + \alpha_1 Z)^2}{r_0^2}\right) \exp\left(-\frac{t'^2}{t_0^2}\right). \quad (21d)$$

The energy conversion efficiency η of third-harmonic light generation is given by

$$\eta = W_3(l) / W_1(0) = \left[\int_{-\infty}^{\infty} dX \int_{-\infty}^{\infty} dY \int_{-\infty}^{\infty} dt' I_3(X, Y, l, t') \right] / \left[\int_{-\infty}^{\infty} dX \int_{-\infty}^{\infty} dY \int_{-\infty}^{\infty} dt' I_1(X, Y, 0, t') \right].$$

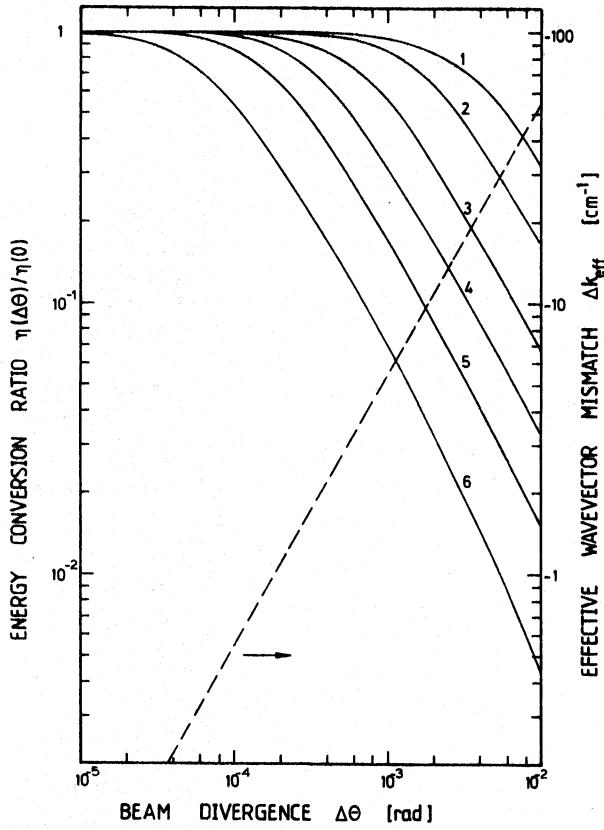


Fig. 4. Reduction of energy conversion efficiency η due to pump-beam divergence $\Delta\theta$. Type-II phase-matching in BaB₂O₄ at wavelength $\lambda_1 = 1.054 \mu\text{m}$. Beam diameter $\Delta d = \infty$. Solid curves: 1 crystal length $l = 1 \text{ mm}$; 2 $l = 2 \text{ mm}$; 3 $l = 5 \text{ mm}$; 4 $l = 1 \text{ cm}$; 5 $l = 2 \text{ cm}$; 6 $l = 5 \text{ cm}$. Dashed curve gives effective wavevector mismatch [12]

For Gaussian input pulses the energy conversion is

$$\eta = \frac{1}{3^{3/2}} \frac{\omega_3^2 l^2 |\chi_{\text{eff}}|^2 I_{10}^2}{n_3 n_{1a} n_{1b} n_{1c} c_0^4 \epsilon_0^2 \cos^4 \alpha_3} \times F(\beta) \frac{\sin^2(\Delta k l/2)}{(\Delta k l/2)^2}. \quad (22)$$

The factor $F(\beta)$ depends on the specific interaction process and is listed in Table 1.

For divergent pump pulses, phase matching $\Delta k' = 0$ is achieved only for the central component of the pulse. The reduction of energy conversion due to the beam divergence $\Delta\theta$ (FWHM) of the pump pulse was analysed in [Ref. 12, Eq. (31)]. The energy conversion ratio $\eta(\Delta\theta)/\eta(0)$ and the effective wavevector mismatch $\Delta k_{\text{eff}}(\Delta\theta)$ [12] are displayed in Fig. 4 for various crystal lengths. The curves apply to type-II phase-matched third-harmonic generation ($\partial \Delta k_{\text{THG}}/\partial \theta = -1.6 \times 10^4 \text{ cm}^{-1}/\text{rad}$). For our experimental situation of $\Delta\theta \approx 5 \times 10^{-4} \text{ rad}$ and $l = 0.72 \text{ cm}$ it is $\eta(\Delta\theta)/\eta(0) \approx 0.65$.

The spectral width $\Delta\tilde{\nu}$ (FWHM) of the pump pulses reduces the energy conversion efficiency, since phase-

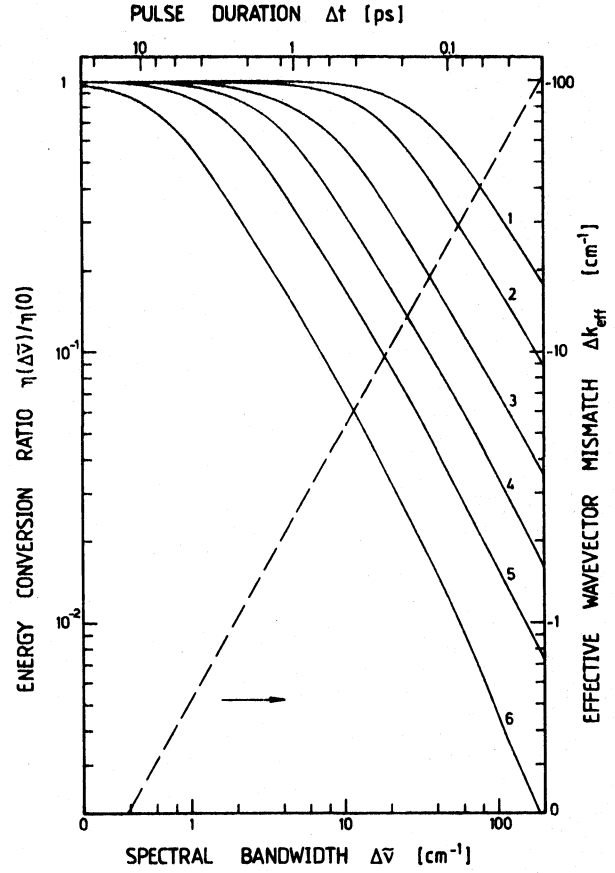


Fig. 5. Reduction of energy conversion efficiency η due to spectral bandwidth $\Delta\tilde{\nu}$ of pump pulse. Type-II phase matching in β -BaB₂O₄. Wavelength $\lambda_1 = 1.054 \mu\text{m}$. Beam diameter $\Delta d = \infty$. Lower abscissa gives spectral width of chirped pulses. Upper abscissa presents pulse duration of Gaussian band-width limited pulses. Solid curves: 1 crystal length $l = 1 \text{ mm}$; 2 $l = 2 \text{ mm}$; 3 $l = 5 \text{ mm}$; 4 $l = 1 \text{ cm}$; 5 $l = 2 \text{ cm}$; and 6 $l = 5 \text{ cm}$. Dashed curve presents effective wavevector mismatch versus spectral bandwidth [12]

matching is achieved only for the central laser frequency. The reduction of the third-harmonic energy conversion efficiency was analysed in [Ref. 12, Eq. (33)]. The energy conversion ratio $\eta(\Delta\tilde{\nu})/\eta(0)$ and the effective wavevector mismatch $\Delta k_{\text{eff}}(\Delta\tilde{\nu})$ are plotted in Fig. 5 for various crystal lengths. The curves belong to type-II phase-matched third-harmonic generation ($\partial \Delta k_{\text{THG}}/\partial \tilde{\nu} = 1.53 \text{ cm}^{-1}/\text{cm}^{-1}$). The lower abscissa represents the spectral width of chirped pulses. (For bandwidth limited pulses $\Delta\tilde{\nu}$ is a factor of three larger [12].) The upper abscissa is valid for the duration of bandwidth limited Gaussian pulses $\{\Delta t = [2 \ln(2)/\pi]/(\Delta\tilde{\nu} c_0) \text{ [25]}\}$. For $\Delta\tilde{\nu} \approx 20 \text{ cm}^{-1}$ (chirped pulses) and $l = 0.72 \text{ cm}$ it is $\eta(\Delta\tilde{\nu})/\eta(0) \approx 0.25$.

The walk-off angle of extraordinary rays reduces the pulse overlap in the case of a finite pump beam diameter Δd (FWHM). The reduction of energy con-

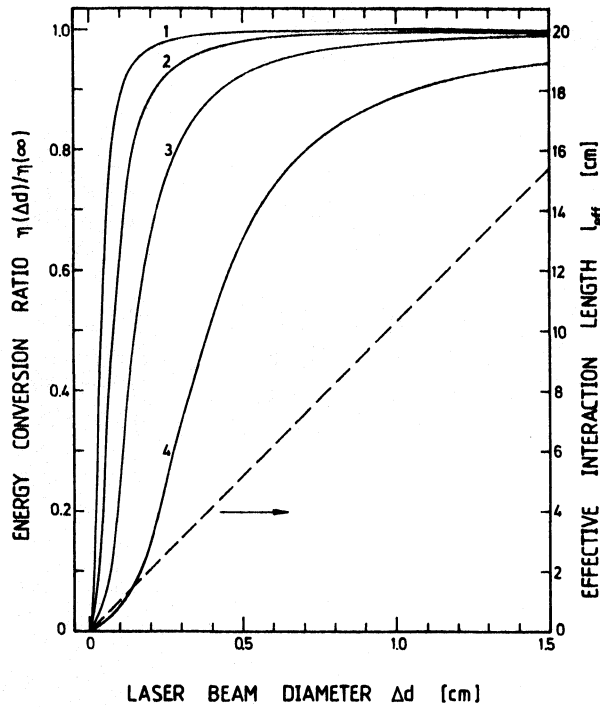


Fig. 6. Reduction of energy conversion efficiency η due to finite pump pulse beam diameter Δd . Type-II phase-matching in β -BaB₂O₄. Wavelength $\lambda_1 = 1.054 \mu\text{m}$. Solid curves: 1 $l = 5 \text{ mm}$; 2 $l = 1 \text{ cm}$; 3 $l = 2 \text{ cm}$; 4 $l = 5 \text{ cm}$. Dashed curve presents effective interaction length [12]

version due to the walk-off angle α_1 was studied in [Ref. 12, Eq. (35)]. In Fig. 6 the energy conversion ratio $\eta(\Delta d)/\eta(\infty)$ versus pump beam diameter Δd is depicted for type-II third-harmonic generation in β -BaB₂O₄. The effective interaction length l_{eff} is included (for a definition, see [12]). For a beam diameter of $\Delta d = 2 \text{ mm}$ and a crystal length of $l = 0.72 \text{ cm}$ the energy conversion ratio is $(\Delta d)/\eta(\infty) \approx 0.93$.

The energy conversion ratio $\eta(\theta)/\eta(\theta_{\text{PM}})$ for $\Delta\theta = 0$, $\Delta\tilde{\nu} = 0$, and $\Delta d = \infty$ is plotted in Fig. 7 [dashed curve 1, Eq. (22)]. The fringe pattern belongs to type-II third-harmonic generation in a β -BaB₂O₄ crystal of 0.72 cm lengths. Several energy conversion ratios $\eta(\theta, \Delta\theta)/\eta(\theta_{\text{PM}}, 0)$ for $\Delta\tilde{\nu} = 0$ (curves 2–6) and $\eta(\theta, \Delta\tilde{\nu})/\eta(\theta_{\text{PM}}, 0)$ for $\Delta\theta = 0$ (curves 7–11) are included in Fig. 7.

Several energy conversion ratios $\eta(\theta, \Delta\theta, \Delta\tilde{\nu})/\eta(\theta_{\text{PM}}, 0, 0)$ for $\Delta d = \infty$ are plotted in Fig. 8 (type-II third-harmonic generation). The left half belongs to $\Delta\theta = 5 \times 10^{-4} \text{ rad}$ and the right half to $\Delta\theta = 10^{-4} \text{ rad}$. The dashed curves belong to bandwidth-limited pulses of $\Delta\tilde{\nu} = 3 \text{ cm}^{-1}$. The solid curves are calculated for various spectral widths $\Delta\tilde{\nu}$ of chirped pulses.

The different group velocities of the ordinary and extra-ordinary pump rays limit their overlap length in

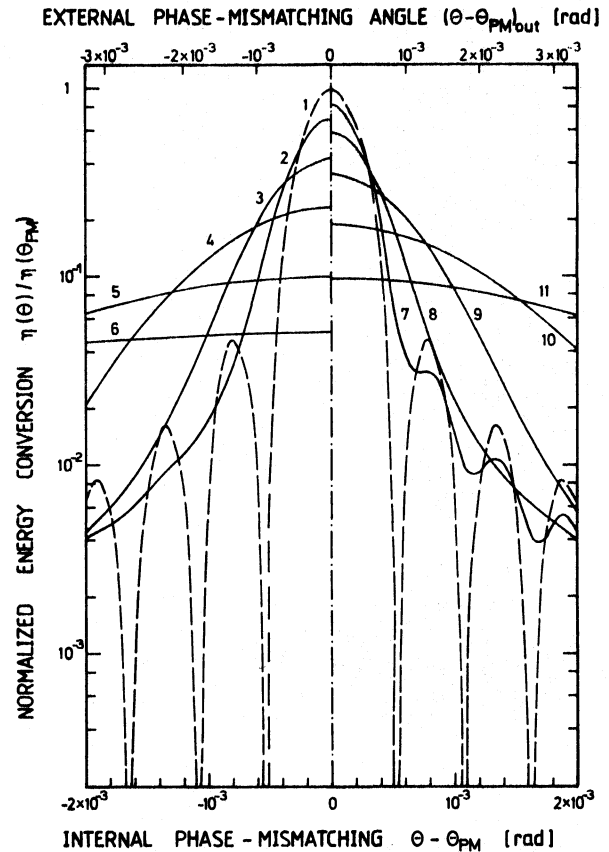


Fig. 7. Normalized energy conversion efficiency versus internal and external phase-mismatching angle. $\theta - \theta_{\text{PM}} \approx (\theta - \theta_{\text{PM}})_{\text{out}}/n_{0,1}$ is the internal mismatch angle. Type-II phase-matching in β -BaB₂O₄. Crystal length $l = 0.72 \text{ cm}$. Wavelength $\lambda_1 = 1.054 \mu\text{m}$. Dashed curve 1: $\Delta\tilde{\nu} = 0$ and $\Delta\theta = 0$. Solid curves 2–6: $\Delta\tilde{\nu} = 0$ with 2 $\Delta\theta = 5 \times 10^{-4} \text{ rad}$, 3 $\Delta\theta = 10^{-3} \text{ rad}$, 4 $\Delta\theta = 2 \times 10^{-3} \text{ rad}$, 5 $\Delta\theta = 5 \times 10^{-3} \text{ rad}$, and 6 $\Delta\theta = 10^{-2} \text{ rad}$. Solid curves 7–11: $\Delta\theta = 0$ with 7 $\Delta\tilde{\nu} = 10 \text{ cm}^{-1}$, 8 $\Delta\tilde{\nu} = 20 \text{ cm}^{-1}$, 9 $\Delta\tilde{\nu} = 40 \text{ cm}^{-1}$, 10 $\Delta\tilde{\nu} = 80 \text{ cm}^{-1}$, and 11 $\Delta\tilde{\nu} = 160 \text{ cm}^{-1}$. Bandwidth-limited pulses are assumed

the crystal. The group refractive index is $n_g = n/[1 - (\tilde{\nu}/n)(\partial n/\partial \tilde{\nu})]$. The time delay per unit length between the ordinary and extraordinary ray at $\lambda_1 = 1.054 \mu\text{m}$ is

$$(\delta t/\delta l)_{0,1} = [n_{g,0,1} - n_{g,e,1}(\theta_{\text{PM}})]/c_0 = 1.54 \text{ ps/cm}$$

in β -BaB₂O₄. The overlap length of a pump pulse of duration Δt (FWHM), $l_{\text{over}} \approx \Delta t/(\delta t/\delta l)_{0,1}$, is plotted in Fig. 9a.

The group-velocity dispersion broaden the duration of the generated third-harmonic light pulses. Without group-velocity dispersion and without pump pulse depletion the third-harmonic duration is $\Delta t_3 = \Delta t/3^{1/2}$ [12]. For type-II phase-matching the time delay between the third-harmonic light and the ordinary ray of the pump pulse is

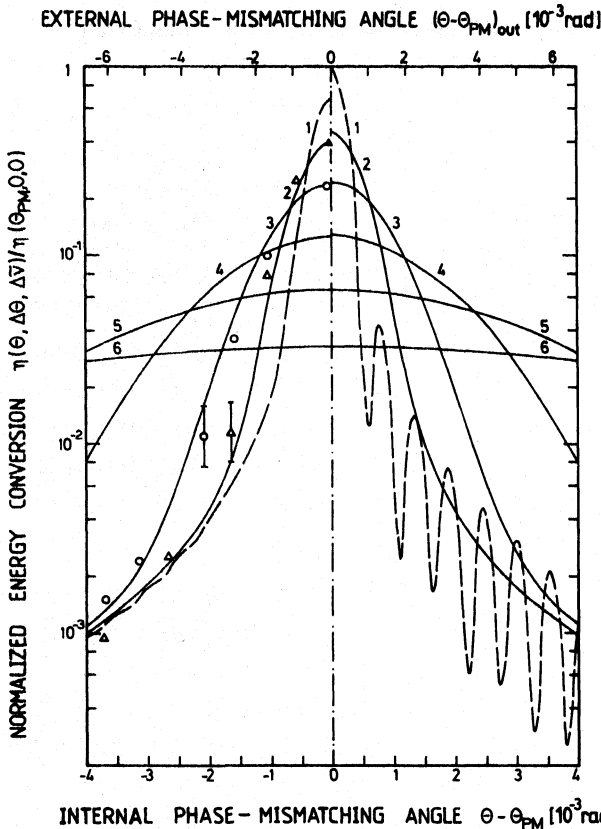


Fig. 8. Normalized energy conversion efficiency versus internal and external phase-mismatching angle. Type-II phase-matching in β -BaB₂O₄. Crystal length $l = 0.72$ cm. Wavelength $\lambda_1 = 1.054$ μ m. Left half: $\Delta\theta = 5 \times 10^{-4}$ rad; right half: $\Delta\theta = 1 \times 10^{-4}$ rad. Curves 1 are bandwidth limited with $\Delta\tilde{\nu} = 3$ cm^{-1} . The other curves are chirped with 2 $\Delta\tilde{\nu} = 10$ cm^{-1} , 3 $\Delta\tilde{\nu} = 20$ cm^{-1} , 4 $\Delta\tilde{\nu} = 40$ cm^{-1} , 5 $\Delta\tilde{\nu} = 80$ cm^{-1} , and 6 $\Delta\tilde{\nu} = 160$ cm^{-1} . The circles belong to $\Delta\tilde{\nu} \approx 20$ cm^{-1} and the triangles belong to $\Delta\tilde{\nu} \approx 10$ cm^{-1} .

$(\delta t/\delta l)_{e3o1} \approx 2.86$ ps/cm ($\lambda_1 = 1.054$ μ m). The third-harmonic pulse duration broadens to $\Delta t_3 = [\Delta t^2/3 + (\delta t/\delta l)_{e3o1}^2 l'^2]^{1/2}$ with $l' = \min(l, l_{\text{over}})$. The approximate third-harmonic pulse duration versus crystal length is shown in Fig. 9b for two pump pulse durations.

2. Experimental

The experimental setup is similar to the arrangement used for phase-matched third-harmonic generation in calcite [12]. The schematic setup is shown in Fig. 10. The pump pulses are generated in a passively mode-locked Nd: phosphate glass laser ($\lambda_1 = 1.054$ μ m). Single picosecond pulses of about 5 ps duration are separated with the Kerr cell shutter. The pulse energy is increased in one or two Nd: phosphate glass amplifiers. The pump pulse spectrum is monitored

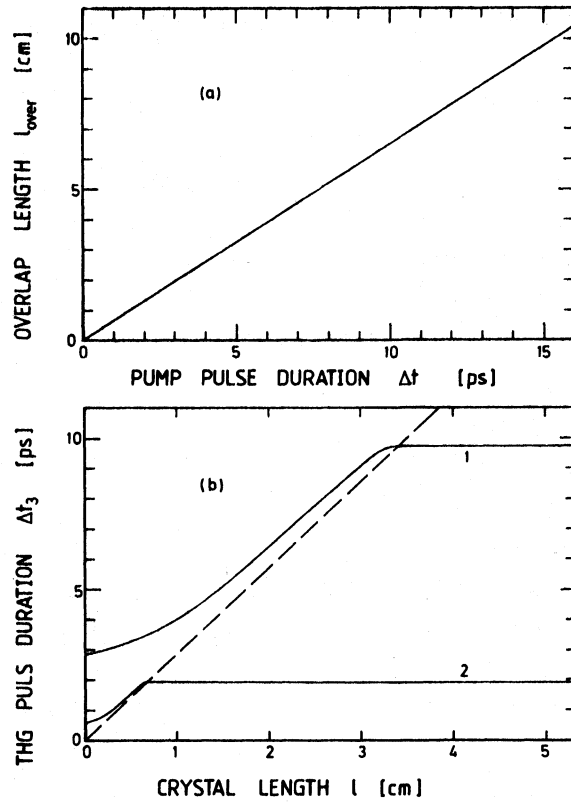


Fig. 9. (a) Overlap length between ordinary and extraordinary ray of pump pulses versus pump pulse duration in β -BaB₂O₄. $\lambda_1 = 1.054$ μ m, $(\delta t/\delta l)_{o1e1} = 1.54$ ps/cm. (b) Pulse duration of generated third-harmonic light in β -BaB₂O₄ versus crystal length. $\lambda_1 = 1.054$ μ m, $(\delta t/\delta l)_{e3o1} = 2.86$ ps/cm. Solid curves: 1 pump pulse duration $\Delta t = 5$ ps; 2 $\Delta t = 1$ ps. Dashed curve: time delay between extraordinary ray at λ_3 and ordinary ray at λ_1 .

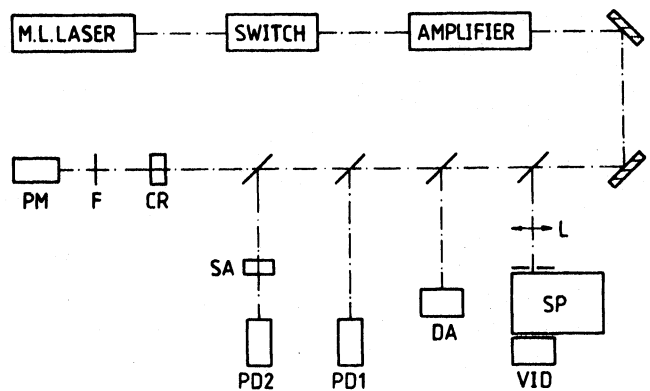


Fig. 10. Experimental setup. (SP; grating spectrometer; VID; vidicon of optical spectrum analyser; L: lens. DA: linear diode array; PD1 and PD2: vacuum photodetectors; SA: saturable absorber for intensity detection; CR: β -BaB₂O₄ crystal; F: filters; PM: photomultiplier)

with a spectrometer and a vidicon system. The beam diameter is measured with a linear diode array system. The input pump pulse peak intensity, I_{10} , is determined by measuring the pulse transmission through a

saturable absorber (Kodak dye No. 9860 in 1,2-dichloroethane [26]). The relevant crystal parameters are $l=0.72$ cm, $\theta_{PM}=47.40^\circ$ (type-II phase-matching), and $\phi=90^\circ$ [27]. Only type-II phase-matched third-harmonic generation is investigated. The generated third-harmonic signal is measured with a photomultiplier. The energy conversion is determined by calibrating the photomultiplier signal, energy $W_3(l)$, to the signal of the photodetector PD1, energy $W_1(0)$. At high pump pulse intensities ($I_{10} \gtrsim 2 \times 10^{10}$ W/cm²) a vacuum photodiode is used to measure the third-harmonic signal.

3. Results

The angular dependence of the generated third-harmonic signal is shown by the data points in Fig. 8 (type-II phase-matched third-harmonic generation). The data belong to $\Delta\theta \approx 5 \times 10^{-4}$ rad and $\Delta d \approx 2$ mm. The spectral widths are $\Delta\tilde{\nu} \approx 10$ cm⁻¹ (triangles) and

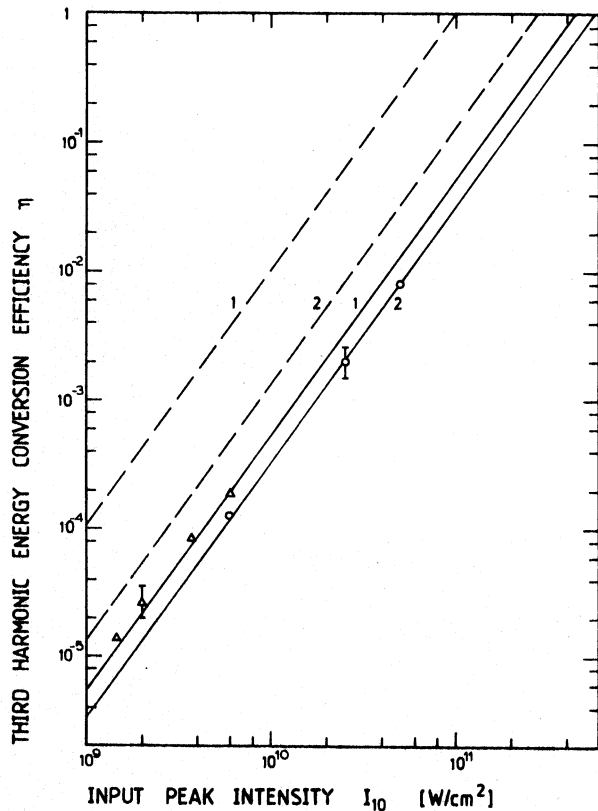


Fig. 11. Energy conversion efficiency of third-harmonic light versus input pump pulse peak intensity. Type-II phase-matching in β -BaB₂O₄. Pump laser wavelength $\lambda_1=1.054$ μ m. Circles and solid curve 1: $\Delta\tilde{\nu} \approx 20$ cm⁻¹, $l=0.72$ cm. Triangles and solid curve 2: $\Delta\tilde{\nu} \approx 10$ cm⁻¹, $l=0.72$ cm. Dashed curves 1 and 2 belong to $\Delta\tilde{\nu} \approx 0$, $\Delta\theta \approx 0$, $\Delta d \rightarrow \infty$ with $l=2$ cm and $l=0.72$ cm, respectively. Curves are calculated with $\chi_{eff} = 1.3 \times 10^{-22}$ m² V⁻², see (22)

$\Delta\tilde{\nu} \approx 20$ cm⁻¹ (circles). The experimental points agree well with the calculated curves.

The maximum energy conversion efficiency ($\theta=\theta_{PM}$) versus input pump pulse intensity is depicted in Fig. 11. The circles ($\Delta\tilde{\nu} \approx 20$ cm⁻¹) and triangles ($\Delta\tilde{\nu} \approx 10$ cm⁻¹) represent the experimental points ($\Delta\theta \approx 5 \times 10^{-4}$ rad, $\Delta d \approx 2$ mm, $l=7.2$ mm). The solid curves are fitted to the experimental data. The fitting parameter is $|\chi_{eff}| = (1.3 \pm 0.2) \times 10^{-22}$ m² V⁻² $= (9.2 \pm 1.4) \times 10^{-15}$ esu (1 esu $= 9 \times 10^8 / 4\pi$ m² V⁻² [21]). The dashed curves belong to $\Delta\theta=0$, $\Delta\tilde{\nu}=0$, $\Delta d=\infty$ with (2) $l=7.2$ mm and (1) $l=2$ cm [see (22)].

In the experiments a third-harmonic conversion efficiency of $\eta \approx 0.008$ has been obtained at an input pump pulse intensity of $I_{10} = 5 \times 10^{10}$ W/cm². The damage threshold of β -BaB₂O₄ crystals is expected to be of the order of 10^{12} W/cm² for picosecond pump pulses of about 5 ps duration. A damage threshold of 1.35×10^{10} W/cm² was reported for Nd:YAG laser pulses of 1 ns duration [4, 7]. The curves in Fig. 11 indicate that very high third-harmonic conversion efficiencies may be obtained for picosecond (and femtosecond) light pulses in BBO (β -BaB₂O₄) well below the damage threshold.

4. Discussion

The type-II phase-matched third-harmonic generation is composed of the direct third-harmonic generation and of four cascading second-order processes. The contributing processes are listed in Table 1. The second-order nonlinear susceptibility components were determined by an analysis of the second-harmonic generation [1, 5–7]. The reported values are [7] $d_{22} = (1.94 \pm 0.22) \times 10^{-12}$ m/V, $d_{11} < 0.1 \times d_{22}$ ($d_{11}=0$ used in the following), and $d_{15} = (1.36 \pm 0.83) \times 10^{-13}$ m/V. A value of d_{33} is still not known. The effective susceptibility of the cascading contributions is found to be $\chi_{eff, cas} = (6.6 \pm 0.8) \times 10^{-23}$ m² V⁻². [Equation (19c) with Table 1 and Table 3, $\phi=90^\circ$, the weak processes $o_1 o_1 \rightarrow e_2 e_1 \rightarrow e_3$ and $o_1 e_1 \rightarrow o_2 o_1 \rightarrow e_3$ are neglected.] The measured effective susceptibility of type-II third-harmonic generation is $|\chi_{eff}| = |\chi_{eff, THG}^{(3)} + \chi_{eff, cas}| = (1.3 \pm 0.2) \times 10^{-22}$ m² V⁻² resulting in $\chi_{eff, THG}^{(3)} = (6.4 \pm 2.8) \times 10^{-23}$ m² V⁻² (same sign of $\chi_{eff, THG}^{(3)}$ and $\chi_{eff, cas}$ is assumed). The effective nonlinear susceptibility values indicate the same magnitude of the cascading processes and the direct third-harmonic generation.

5. Conclusions

Energy conversion efficiencies up to 1% have been achieved by type-II phase-matched third-harmonic generation in β -BaB₂O₄ with picosecond pump pulses

Table 3. Effective second- and third-order nonlinear susceptibilities of β -BaB₂O₄ (point group 3). Angles are defined in Fig. 1

Process	χ_{eff}
Second-harmonic generation	$\chi_{\text{eff,SHG}}^{(2)}(\omega_1 + \omega_1 \rightarrow \omega_2)$
oo \rightarrow e	$[-d_{11} \cos(3\phi) + d_{22} \sin(3\phi)] \cos(\theta + \alpha_2) - d_{15} \sin(\theta + \alpha_2)$
oo \rightarrow o	$-d_{11} \sin(3\phi) + d_{22} \cos(3\phi)$
oe \rightarrow e	$[d_{11} \sin(3\phi) + d_{22} \cos(3\phi)] \cos(\theta + \alpha_1) \cos(\theta + \alpha_2)$
oe \rightarrow o	$[-d_{11} \cos(3\phi) + d_{22} \sin(3\phi)] \cos(\theta + \alpha_1) - d_{15} \sin(\theta + \alpha_1)$
ee \rightarrow e	$[d_{11} \cos(3\phi) - d_{22} \sin(3\phi)] \cos(\theta + \alpha_2) \cos^2(\theta + \alpha_1) + d_{33} \sin(\theta + \alpha_2) \sin^2(\theta + \alpha_1)$ $+ d_{15} \cos(\theta + \alpha_1) [\sin(\theta + \alpha_2) \cos(\theta + \alpha_1) - 2 \cos(\theta + \alpha_2) \sin(\theta + \alpha_1)]$
ee \rightarrow o	$[d_{11} \sin(3\phi) + d_{22} \cos(3\phi)] \cos^2(\theta + \alpha_1)$
Frequency mixing	$\chi_{\text{eff,FM}}^{(2)}(\omega_1 + \omega_2 \rightarrow \omega_3)$
oo \rightarrow e	$[-d_{11} \cos(3\phi) + d_{22} \sin(3\phi)] \cos(\theta + \alpha_3) - d_{15} \sin(\theta + \alpha_3)$
oo \rightarrow o	$-d_{11} \sin(3\phi) + d_{22} \cos(3\phi)$
oe \rightarrow e	$[d_{11} \sin(3\phi) + d_{22} \cos(3\phi)] \cos(\theta + \alpha_2) \cos(\theta + \alpha_3)$
oe \rightarrow o	$[-d_{11} \cos(3\phi) + d_{22} \sin(3\phi)] \cos(\theta + \alpha_2) - d_{15} \sin(\theta + \alpha_2)$
ee \rightarrow e	$[d_{11} \cos(3\phi) - d_{22} \sin(3\phi)] \cos(\theta + \alpha_1) \cos(\theta + \alpha_2) \cos(\theta + \alpha_3)$ $+ d_{33} \sin(\theta + \alpha_1) \sin(\theta + \alpha_2) \sin(\theta + \alpha_3)$ $+ d_{15} [\cos(\theta + \alpha_1) \cos(\theta + \alpha_2) \sin(\theta + \alpha_3) - \cos(\theta + \alpha_1) \sin(\theta + \alpha_2) \cos(\theta + \alpha_3)]$ $- \sin(\theta + \alpha_1) \cos(\theta + \alpha_2) \cos(\theta + \alpha_3)]$
ee \rightarrow o	$[d_{11} \sin(3\phi) + d_{22} \cos(3\phi)] \cos(\theta + \alpha_1) \cos(\theta + \alpha_2)$
Direct third-harmonic generation	$\chi_{\text{eff,THG}}^{(3)}(\omega_1 + \omega_1 + \omega_1 \rightarrow \omega_3)$
ooo \rightarrow e	$-[\chi_{15} \sin(3\phi) + \chi_{10} \cos(3\phi)] \sin(\theta + \alpha_3)$
ooe \rightarrow e	$\frac{1}{3} \chi_{11} \cos(\theta + \alpha_3) \cos(\theta + \alpha_1) + [\chi_{10} \sin(3\phi) - \chi_{15} \cos(3\phi)] \sin(2\theta + \alpha_1 + \alpha_3)$ $+ \chi_{16} \sin(\theta + \alpha_3) \sin(\theta + \alpha_1)$
oee \rightarrow e	$\frac{2}{3} [\chi_{10} \cos(3\phi) + \chi_{15} \sin(3\phi) \cos(\theta + \alpha_3) \sin(2\theta + 2\alpha_1)]$

of a Nd:glass laser. Conversion efficiencies up to the 10% region are expected for more powerful picosecond pump pulses well below the damage threshold. Comparing the third-harmonic generation in BBO with the third-harmonic generation in calcite reveals the favorite parameters of β -BaB₂O₄: The effective nonlinear susceptibility χ_{eff} (type-II) is about a factor of 40 higher, the walk-off angle is nearly a factor of 2 smaller, and the half-width of the phase-matching curve (Fig. 7, curve 1) is a factor of 1.35 wider (same crystal thickness).

Acknowledgements. The authors thank Th. Ascherl for technical assistance and the Rechenzentrum of our University for disposal of computer time. P.Q. is very grateful to the Alexander von Humboldt Stiftung for a fellowship.

References

- C. Chen, B. Wu, G. You, A. Jiang, Y. Huang: in Dig. Tech. Papers, XIII IQEC 1984, paper MCC5, p. 20
- C. Chen, B. Wu, A. Jiang, G. You: Sci. Sinica (Ser. B) **28**, 235 (1985)
- K. Kato: IEEE J. QE-22, 1013 (1986)
- C. Chen, Y.X. Fan, R.C. Eckardt, R.L. Byer: CLEO 1986, paper THQ4, p. 322
- Y. Ishida, T. Yajima: Opt. Commun. **62**, 197 (1987)
- P. Lokai, B. Burghardt, D. Basting, W. Mückenheim: Laser and Optoelektronik **19**, 296 (1987)
- H. Schmidt, R. Wallenstein: Laser and Optoelektronik **19**, 302 (1987)
- K. Miyazaki, H. Sakai, T. Sato: Opt. Lett. **11**, 797 (1986)
- R.S. Adhav, S.R. Adhav, J.M. Pelaprat: Laser Focus **23**, 88 (September 1987)
- S.A. Akhmanov, L.B. Meisner, S.T. Parinov, S.M. Saltiel, V.G. Tunkin: Sov. Phys. JETP **46**, 898 (1978)
- C.C. Wang, E.L. Baardsen: Appl. Phys. Lett. **15**, 425 (1969)
- A. Penzkofer, F. Ossig, P. Qiu: To be published
- M. Born, E. Wolf: *Principles of Optics* (Pergamon, Oxford 1980)
- D. Eimerl: IEEE J. QE-23, 575 (1987)
- R. Piston: Laser Focus **14**, 66 (July 1978)
- K.W. Kirby, L.G. DeShazer: J. Opt. Soc. Am. B **4**, 1072 (1987)
- P.N. Butcher: Nonlinear Optical Phenomena, Bulletin 200, Engineering Experiment Station, Ohio State University (Columbus, Ohio 1965)
- Y.R. Shen: *The Principles of Nonlinear Optics* (Wiley, New York 1984)
- M. Schubert, B. Wilhelmi: *Nonlinear Optics and Quantum Electronics* (Wiley, New York 1986)
- J.A. Armstrong, N. Bloembergen, J. Ducuing, P.S. Pershan: Phys. Rev. **127**, 1918 (1962)
- R.W. Minck, R.W. Terhune, C.C. Wang: Appl. Opt. **5**, 1595 (1966)
- J.E. Midwinter, J. Warner: Brit. J. Appl. Phys. **16**, 1135 (1965)
- J.E. Midwinter, J. Warner: Brit. J. Appl. Phys. **16**, 1667 (1965)
- D.A. Kleinman: Phys. Rev. **126**, 1977 (1962)
- J. Herrmann, B. Wilhelmi: *Laser für ultrakurze Lichtimpulse* (Physik Verlag, Weinheim 1984) p. 84
- A. Penzkofer, D. von der Linde, A. Laubereau: Opt. Commun. **4**, 377 (1972)
- The β -BaB₂O₄ crystal is supplied from the Fujian Institute of Research on the Structure of Matter, Academia Sinica, Fuzhou, Fujian, China

Note added in proof. In a recent paper [28] convincing arguments are given that the trigonal crystal β -BaB₂O₄ is of higher symmetry. The space group is claimed to be $R3c$ giving a point group symmetry of $3m$. In this case it is $d_{11}=0$ and $\chi_{15}=0$ (Tables 2 and 3). With this setting all the text remains valid for $R3c$ symmetry. It should be mentioned that in this paper the IRE convention [29] is used for defining the crystallographic axes [30], i.e. for $R3c$ symmetry the mirror plane m is perpendicular to x . In [1-9,28] $m \perp y$ is used. This different assignment interchanges the susceptibility components d_{11} and

d_{22} (d_{22} in this paper is equal to d_{11} in [1-9,28] and vice versa). The other d -components remain unchanged.

28. D. Eimerl, L. Davis, S. Velsko, E.K. Graham, A. Zalkin: J. Appl. Phys. **62**, 1968 (1987)
29. J.G. Brainerd et al.: Standards on piezoelectric crystals. Proc. IRE **37**, 1378 (1949)
30. S. Singh: Nonlinear Optical Materials, in *CRC Handbook of Lasers*, ed. by R.J. Pressley (The Chemical Rubber Co., Cleveland, Ohio 1971) p. 489